NANO LETTERS

Letter

pubs.acs.org/NanoLett

Polarization Switchable Diffraction Based on Subwavelength Plasmonic Nanoantennas

Yunuen Montelongo,*[,†] Jaime O. Tenorio-Pearl,[†] William I. Milne,[†,‡] and Timothy D. Wilkinson[†]

[†]Electrical Engineering Division, Department of Engineering, University of Cambridge, 9 JJ Thomson Avenue, Cambridge CB3 0FA, United Kingdom

[‡]Display Research Lab, Department of Information Display, Kyung Hee University, Seoul 130701, South Korea

Supporting Information

ABSTRACT: We prove theoretically and experimentally the concept of polarization holography by producing visible diffraction through radiation emitted by plasmonic nanoantennas. We show a methodology to selectively activate the nanoantenna emission by controlling the orientation of the electric field of a beam. Additionally, we demonstrate that it is possible to superpose two independent transverse nanoantennas in the same plane without producing interference in their radiated field. Hence, we introduce an alternative view to the traditional concept of holography where fringes (or diffractive units) are band-limited to half the wavelength.

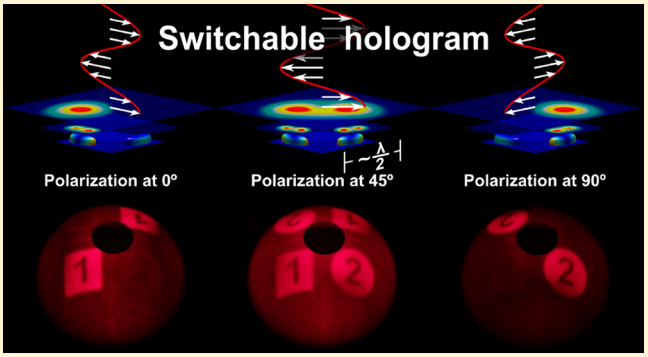

KEYWORDS: *Plasmonics, nanoantenna, holography, diffraction, polarization, switching*

Plasmonic nanoantennas have been of interest for their unique optical properties.[1] Antennas in general are metallic structures that can receive and radiate electromagnetic fields. This arises when the charges in the material resonate along the structure. When the charge movement resonates with the electromagnetic field a further emission occurs. Therefore, dimensions and shapes dictate the characteristics of the emission. For instance, a perfectly conducting rod with a negligible skin depth will have resonances when the length of the long axis is equal to any multiple of half the wavelength. In contrast, when the polarization is rotated toward the short axis the resonant conditions change. A crucial criterion to consider is that antennas do not scale linearly across the whole spectra. The reason for this is that at short wavelengths the skin depth is of comparable size to the antenna. Hence, radiation penetrates the metal and causes oscillations of the free-electron gas within. According to literature[2,3] the effective resonant wavelength in the nanoantenna can be reduced to a fraction of the size. Although this disproportion of scalability might seem problematic, a nanoantenna with reduced dimensions allows the superposition of multiple independent diffractive units on subwavelength areas. In contrast with typical dielectric subwavelength nanostructures that have a uniform behavior regardless of size or shape, plasmonic nanostructures can be engineered to enhance a specific wavelength and polarization. More importantly, orthogonal polarizations can be manipulated independently without losing spacial resolution. In this work, we show a theoretical and an experimental approach to achieve visible holograms through the coherent excitation of plasmons of a dipolar nanoantenna as a single diffractive unit. Additionally, we challenge the traditional concept of a hologram by superposing two different antennas with orthogonal polarizations within a distance smaller than half the wavelength.

A traditional hologram fabricated by means of interference consists of diffractive fringes of sizes over half the wavelength. Using Gabor's principle, the amount of information recorded in a hologram is band-limited by the wavelength.[4] A digital hologram can be designed artificially by sampling the fringes with a grid of diffractive units. Following the Nyquist−Shannon sampling theorem, the complete hologram can be reproduced by sampling the hologram with diffractive units spaced by half the wavelength. It has been proposed that subwavelength dielectric structures only alter the effective medium without affecting the diffraction pattern.[5] An expansion of the effective medium approach was also suggested for metals.[6] The effective medium theory can simplify the design of a hologram, but the effect of an individual nanostructure is not considered. Alternatively, a single carbon nanotube as a diffractive unit has been demonstrated in holography.[7] In contrast to the effective medium theory, the scattering of a subwavelength structure was used as a diffractive unit. Interestingly, when these nanostructures have a large scattering cross-section, the diffraction effect is highly enhanced.[8,9] It is not uncommon for a metallic nanostructure to scatter over five times more light

Received: October 25, 2013
Revised: November 24, 2013
Published: November 27, 2013

   dx.doi.org/10.1021/nl4039967 | *Nano Lett.* 2014, 14, 294−298

than that calculated purely from its geometrical cross-section.[10] Another completely different approach is selectively and simultaneously illuminating different nanostructures with a predefined field to superpose their radiation as eigenmodes, hence patterns of few pixels can be reconstructed. This method does not consider subwavelength grids between diffractive nanostructures and is not suitable for direct laser lighting.[11]

Switching Plasmonics. Our approach is based on the field emission of sampled nanoantennas. In order to create a diffractive effect, it is necessary for electrons in all of the nanoantennas to resonate in phase with a coherent source. Hence, when a laser beam is applied normal to the hologram plane, it is possible to induce emissions in phase. However, only those nanoantennas oriented in the direction of the electric field will emit. This means that by changing the incident light polarization the nanoantennas can be "switched on" or "switched off". To take advantage of this we have superposed two transverse polarizations at a subwavelength distance. This is based on the assumption that two off-axes dipolar antennas with transverse polarizations have minimal coupling. In the case of particles, it has been suggested that dipolar coupling is negligible when the distance between them is larger than ~3 times the radii.[12] To avoid the interaction between transverse polarizations we have chosen to place two nanoantennas in an "L" shape separated by a fixed distance. This task would be impossible with typical antennas if the pitch of the sampled hologram was the same as the antenna length. However, in the case of optical nanoantennas, this is easily achievable with a wide separation between them. In contrast, if coupling is required, a "T" shape can produce an anisotropic interaction between the nanoantennas in one of the polarizations.

The steps to produce a hologram start with two arbitrary and independent designs either in two-dimensions or three-dimensions. Each of those designs represents the reconstructions of the relevant polarization. The diffraction pattern must then be obtained by using a retrieving algorithm similar to a computer-generated hologram.[7] Once the diffraction pattern is obtained, the sampling process should be performed. In this step, the two independent holograms have to be sampled giving the two transverse nanoantennas. A square grid is optimum due to its geometrical match with the two transverse polarizations. The last step in the hologram design consists of merging the two holograms into a single one. To maximize the interantenna distance, each hologram has to be shifted by half the sampling pitch in both directions. The displacement between antennas shifts only the phase of the reconstruction without altering the intensity pattern. Figure 1 shows the design process and the final "L" shape formed by both transverse nanoantennas.

In order to prove the concept, first the nanoantenna characterization had to be performed. The material chosen was silver because of its favorable plasmonic properties in the visible spectrum.[13] The optimum parameters for the nanoantennas were calculated according to literature,[3] simulations, and experiments. The nanostructure chosen was a nanorod with dimensions of about 60 nm in diameter and 170 nm in length. This nanoantenna showed a strong emission for the red wavelength (650 nm) with a polarization in the direction of its long axis and no interaction with the transverse polarization. We tested experimentally our approach by evaluating each hologram in the far field. The target of the two transverse polarizations consisted of two independent images, one containing a square with an inscribed number "1" and the other containing a circle with an inscribed number "2". The

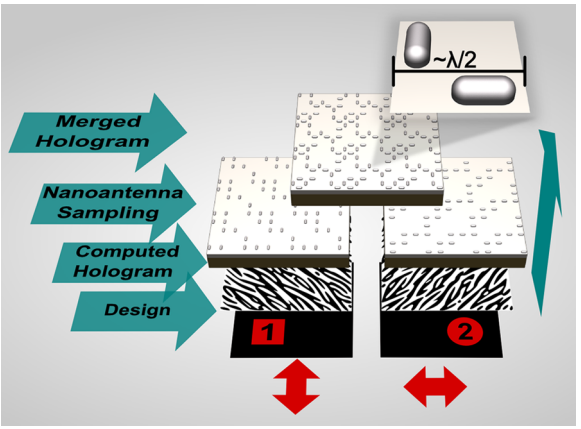

Figure 1. The four steps to generate a hologram consist of the digital creation of two independent images for each polarization, the retrieval of independent diffraction patterns, the nanoantenna sampling of the fringes, and finally the blending of both sampled designs. Through this process, the characteristic "L" shape of transverse nanoantennas is formed in the hologram.

independent holograms that reconstruct these images were retrieved using the Gerber–Saxton algorithm.[14] A computer program was developed to generate two arrays of 3750 × 3750 nanoantennas with a pitch of 390 nm. Finally the two sampled holograms were merged into a single overall hologram pattern.

Methods. The nanoantennas were fabricated on top of a 200 nm silicon dioxide layer on a standard silicon wafer. The substrate was spin-coated with high-resolution positive poly-(methyl methacrylate) 950K resist and electron beam lithography was used to define the nanoantenna structures. After exposure, the samples were developed in a methyl isobutyl ketone/isopropyl alcohol solution with a 1:3 composition. Finally, silver was thermally evaporated and lifted off to remove the unwanted residual metal areas. The total number of nanoantennas created was 6.25×10^6 distributed over an area of 2.13 mm^2. Although the final array of nanoantennas was laid on top of a dielectric silicon dioxide layer, the silicon substrate obstructed the transmitted light. In Figure 2, scanning electron microscopy pictures at different magnifications show the results obtained through this process. The two transverse nanoantennas in an "L" shape form a large array with a profile similar to a weave. The dimensions of the nanorods are uniform but some roughness can be observed on the surface of the nanoantennas.

Results. Figure 3 shows the simulations and the tested reconstructed holograms for polarizations at 0, 45, and 90°. The simulation shows the intensity of the field at the boundaries of the two transverse nanoantennas from a single diffractive unit of 390 nm × 390 nm. Additionally, it shows the field intensity in two different planes, one at 20 nm and the other at 120 nm from the top of the nanoantenna. The intensity at the boundaries (and the first plane) shows the dipolar behavior while the second plane shows the radiated far-field. It can be observed that the interaction occurs mainly when the electric field of the light is oriented in the direction of the long axis, so the radiated pattern in transverse polarization is negligible. It is interesting to note that when the polarization is oriented at 45° a resonance in both antennas is equally induced. Simulations were performed using the boundary element method as shown in literature.[15] The real reconstruction is observed simply by shining a low intensity laser diode in

dx.doi.org/10.1021/nl4039967 | Nano Lett. 2014, 14, 294–298

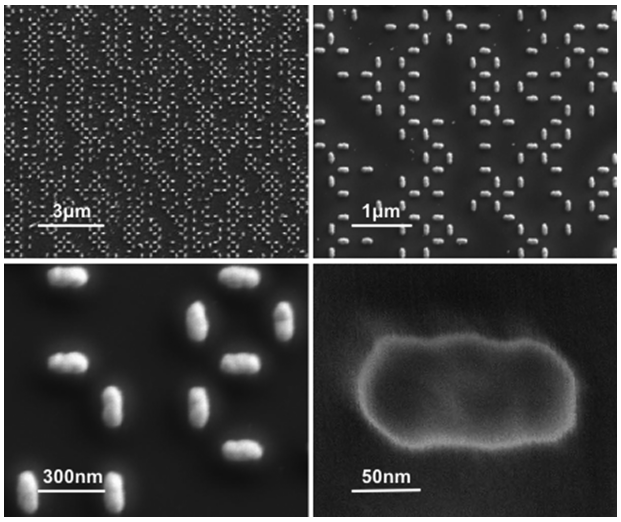

Figure 2. Four different magnifications of a section of the hologram. A distinctive weave profile is formed when the two transverse nanoantennas are placed off-axes. Dimensions are highly uniform along the whole sample, but some roughness is observed at high magnification on the nanoantennas.

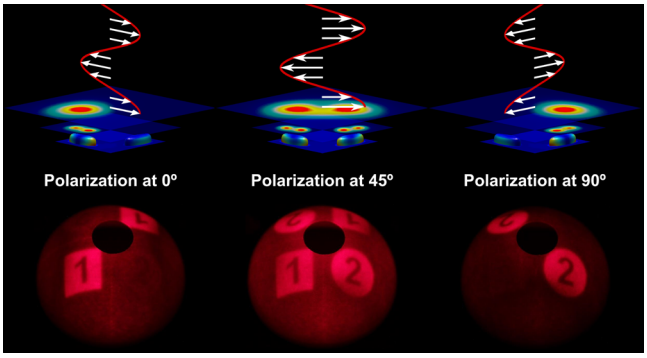

Figure 3. Simulations and experimental results for two independent holograms at 0, 45, and 90°. The simulations map the intensities of the pointing vector on two different planes (20 and 120 nm from the top of the nanoantenna). The results show the reconstruction of two independent polarization holograms. Nanoantennas only resonate when the electric field is oriented in the direction of its corresponding long axis. When the electric field is at 45°, both nanoantennas produce emission simultaneously with half the intensity.

a direction normal to the hologram plane. The image is switched off just by rotating the laser along the normal. Alternatively, the laser can be kept steady at 45° while a polarizer attenuates one of the components according to its orientation. The pictures in the lower part of Figure 3 show the projected image on a diffusive sphere for the excitation of the two independent nanoantenna holograms. In addition, the polarization at 45° image shows the excitation of both polarizations producing the two images simultaneously. It is interesting to note that the background noise of the reconstruction draws the antenna radiation pattern as an envelope in the whole sphere. This pattern represents an important characteristic of a diffractive antenna array. In this case, two opposite lobes are imaged in the direction of the axis for each excited antenna. Another relevant observation is that the intensity does not decrease at large diffractive angles. In contrast to diffractive optical elements based on embossing or relief,[16] nanoantennas can be highly omnidirectional,[17] therefore holograms can achieve a wide field of view with a uniform angular intensity distribution. Our hologram was sampled with a square grid of 390 nm pitch and illuminated with a laser of 650 nm of wavelength, which produced a field of view of 112.8°.

Gray-scale images can also be reproduced with the same methodology. Figure 4 shows the projected hologram of a

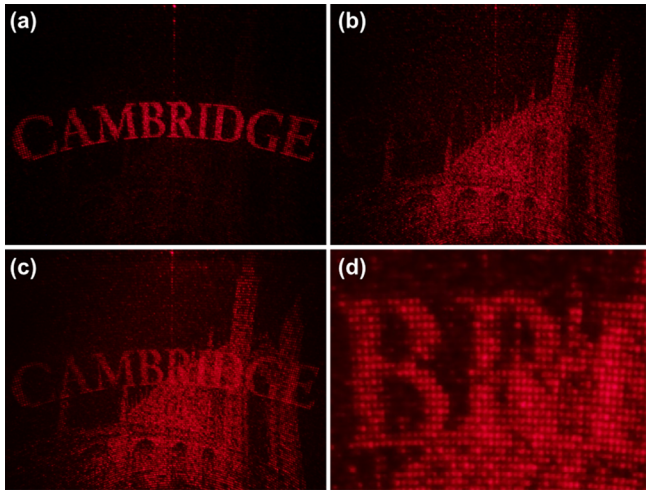

Figure 4. Reconstruction of a gray scale hologram with two independent images for both polarizations. The two transverse polarizations (a) and (b) show minimal leakage. When both transverse nanoantennas are exited with an electric field at 45° there is no interference between them (c). Whether both nanoantennas resonate in phase or not, their radiation is always additive because both emissions have orthogonal polarizations. The reconstruction in (d) is highly resolved and it is possible to differentiate the pixels of the original image.

multilevel intensity image of 250 × 250 pixels on a flat surface. The reconstruction was computed for projection onto a spherical surface (the dynamic projection is shown in a video as Supporting Information), so the wide field of view produces distortion at the outer regions of the image. In this case, the two independent images were the word "Cambridge" and a photo of Kings College's Chapel, Cambridge. Figure 4c shows the reconstruction of the emission of the two transverse nanoantennas. In contrast with the reconstructions in Figure 3, here the two independent images overlap. Interestingly, the two transverse polarizations do not interfere and therefore the intensity is always additive. The same applies for circularly polarized light with the difference being that both orthogonal electric fields are out of phase by $\pi/2$. However, it is possible to produce interference between both orthogonal nanoantennas by rotating the polarization of one of the components by $\pi/2$. One important advantage of creating a polarization-dependent diffractive element is that both polarizations can be controlled independently. Whether the beam is polarized or not, the radiated light will always maintain the polarization signature of the resonant nanostructure. This demonstrates that the amount of information encoded in the hologram can be doubled if the two transverse electric fields are diffracted independently. Figure 4d shows a magnified version of the central region of the projection using both polarizations incident simultaneously. Pixels of the reconstructed images appear clear and highly resolved.

dx.doi.org/10.1021/nl4039967 | Nano Lett. 2014, 14, 294−298

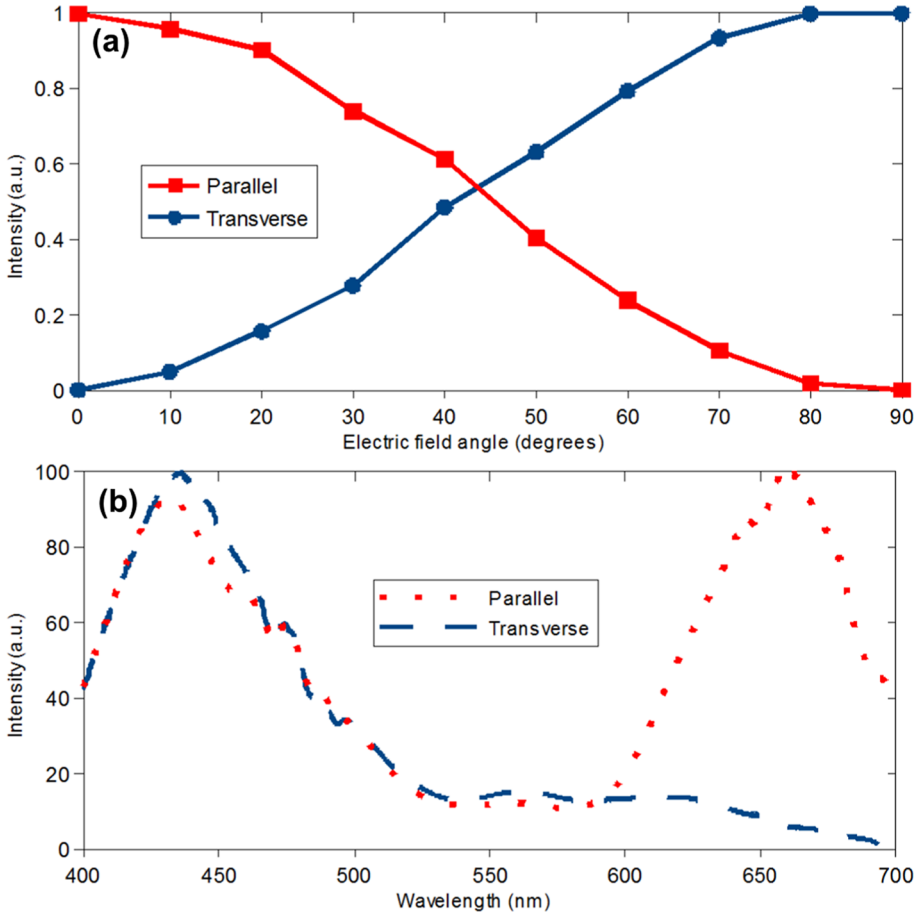

Figure 5. Emission characteristics of both polarizations. (a) Intensity relation of the two diffracted emissions for a wavelength of 650 nm and an electric field oriented at different angles. The emissions of parallel and transverse polarizations were measured simultaneously. (b) Measurement of the intensity difference at different polarization angles. The parallel and transverse polarizations were measured from the two independent diffracted polarizations. The antenna has a resonant peak at 435 nm in the short axis and one at 660 nm in the long axis.

Discussion. The relation between diffracted intensities in the far field produced by both polarizations can be found by projecting the component of the electric field vector in the nanoantenna resonant axis. The solution is given by $I_i \cos^2(\theta)$, where I_i is the intensity of the incident beam and θ is the angle between the resonant axis and the electric field vector. This solution is similar to that for a pair of polarisers, known as Malu's law, but in this case the solution represents the diffraction produced by radiated light. We have proven this by simultaneously measuring the intensities of both diffracted images (see Figure 5a). The polarization extinction ratio in our experiments is minimal, and hence it is not even possible to distinguish if it belongs to the polarizer imperfection, transverse resonances, or plasmonic coupling between antennas. The polarizer used had an intrinsic leakage of about 1%, but according to simulations the transverse resonance of the silver nanoantenna used is about 5% with respect to the parallel resonance. However, the transverse resonance does not necessarily radiate in an omnidirectional way, and therefore its intensity might be even dimer in the far-field (this transverse resonance can be decreased even further with optimization). Coupling between nanoantennas is negligible according to simulations and literature.[12] The total backscattered efficiency measured at the far-field with a 650 nm beam was around 3% with respect to the zero order. However, this is not a clear picture of the real diffraction efficiency because our samples couple most of the light inside the silicon dioxide layer that then gets trapped or absorbed by the silicon wafer. Catchpole et al. showed that hemispherical shapes couple around 90% of the light into the substrate.[18] Furthermore, silver nanoparticles at these dimensions have a negligible absorption compared with their scattering. Through an alternative measurement of the zero order, it was found that about 17% of the light incident on our samples was scattered (considering minimal absorption). This figure seems to be more reasonable if the total geometrical fill factor of the nanoantennas is about 3% and the scattering cross-section enhances the diffraction by a factor of 5. A similar effect would occur for backscattering diffraction if the silicon dioxide was replaced with other dielectric substrates. Hence, we can predict that the efficiency can be highly enhanced by using forward scattering with a transmissive substrate and by matching the refractive index of the substrate. An experiment with white light was also performed to obtain the spectral characteristics. The graph in Figure 5b shows the results obtained by measuring the diffracted images in both polarizations. The two resonant peaks appear according to the orientation of the nanoantennas. The short axis resonance produces a peak in wavelength of about 435 nm while the long axis has a maximum resonance of about 660 nm. In addition, the long axis produces an anomalous second peak at 430 nm. This anomalous resonance has been reported in literature and it has been attributed to surface plasmon polaritons in the

dx.doi.org/10.1021/nl4039967 | Nano Lett. 2014, 14, 294−298

presence of the substrate.[19] Substrates can dramatically change the behavior of particles with respect to free space models.[20] Another possible reason is the interference between the reflective and backscattered waves.

Conclusion. We have shown a theoretical approach to control the emission of nanostructures by exploiting the plasmonic properties of anisotropic nanostructures. Hence, we have fabricated a switchable hologram capable of reconstructing high resolution images over a wide field of view. Additionally, we have proven experimentally that it is possible to superpose two independent transverse polarizations in a subwavelength distance without producing cross-talk. Through this procedure the bandwidth of a hologram is expanded by a factor of 2. Following this principle, it is possible to fabricate any kind of diffractive optical element where independent polarization control is required.

■ ASSOCIATED CONTENT

Supporting Information

Video of a dynamic holographic switching. This material is available free of charge via the Internet at http://pubs.acs.org.

■ AUTHOR INFORMATION

Corresponding Author

*E-mail: ym283@cam.ac.uk.

Author Contributions

The manuscript was written through contributions of all authors. All authors have given approval to the final version of the manuscript.

Notes

The authors declare no competing financial interest.

■ ACKNOWLEDGMENTS

Y.M. and J.O.T.-P. would like to acknowledge financial support from the Cambridge Overseas Trust and the Mexican National Council on Science and Technology (CONACyT).

■ REFERENCES

(1) Maier, S. A. *Plasmonics: Fundamentals and Applications*; Springer: New York, 2007.

(2) Bryant, G. W.; Garcia de Abajo, F. J.; Aizpurua, J. Mapping the Plasmon Resonances of Metallic Nanoantennas. *Nano Lett* **2008**, *8*, 631−636.

(3) Novotny, L. Effective Wavelength Scaling for Optical Antennas. *Phys. Rev. Lett.* **2007**, *98*, 266802.

(4) Gabor, D. A New Microscopic Principle. *Nature* **1948**, *161*, 777−778.

(5) Yu, W.; Takahara, K.; Konishi, T.; Yotsuya, T.; Ichioka, Y. Fabrication of Multilevel Phase Computer-Generated Hologram Elements Based on Effective Medium Theory. *Appl. Opt.* **2000**, *39*, 3531−3536.

(6) Larouche, S.; Tsai, Y.-J.; Tyler, T.; Jokerst, N. M.; Smith, D. R. Infrared Metamaterial Phase Holograms. *Nat. Mater.* **2012**, *11*, 450−454.

(7) Montelongo, Y.; Butt, H.; Butler, T.; Wilkinson, T. D.; Amaratunga, G. A. J. Computer Generated Holograms for Carbon Nanotube Arrays. *Nanoscale* **2013**.

(8) Butt, H.; Montelongo, Y.; Butler, T.; Rajesekharan, R.; Dai, Q.; Shiva-Reddy, S. G.; Wilkinson, T. D.; Amaratunga, G. A. J. Carbon Nanotube Based High Resolution Holograms. *Adv. Mater.* **2012**, *24*, OP331−OP336.

(9) Butt, H.; Butler, T.; Montelongo, Y.; Rajesekharan, R.; Wilkinson, T. D.; Amaratunga, G. A. J. Continuous Diffraction Patterns from Circular Arrays of Carbon Nanotubes. *Appl. Phys. Lett.* **2012**, *101*, 251102−251102−4.

(10) Evanoff, D. D.; Chumanov, G. Size-Controlled Synthesis of Nanoparticles. 2. Measurement of Extinction, Scattering, and Absorption Cross Sections. *J. Phys. Chem. B* **2004**, *108*, 13957−13962.

(11) Kosmeier, S.; De Luca, A. C.; Zolotovskaya, S.; Di Falco, A.; Dholakia, K.; Mazilu, M. Coherent Control of Plasmonic Nanoantennas Using Optical Eigenmodes. *Sci. Reports* **2013**, 3.

(12) Khunsin, W.; Brian, B.; Dorfmüller, J.; Esslinger, M.; Vogelgesang, R.; Etrich, C.; Rockstuhl, C.; Dmitriev, A.; Kern, K. Long-Distance Indirect Excitation of Nanoplasmonic Resonances. *Nano Lett.* **2011**, *11*, 2765−2769.

(13) West, P. r.; Ishii, S.; Naik, G. v.; Emani, N. k.; Shalaev, V. m.; Boltasseva, A. Searching for Better Plasmonic Materials. *Laser Photonics Rev.* **2010**, *4*, 795−808.

(14) Gerchberg, R. W.; Saxton, W. O. A Practical Algorithm for the Determination of the Phase from Image and Diffraction Plane Pictures. *Optik* **1972**, *35*, 237−246.

(15) Hohenester, U.; Trügler, A. MNPBEM − A Matlab Toolbox for the Simulation of Plasmonic Nanoparticles. *Comput. Phys. Commun.* **2012**, *183*, 370−381.

(16) Hessler, T.; Rossi, M.; Kunz, R. E.; Gale, M. T. Analysis and Optimization of Fabrication of Continuous-Relief Diffractive Optical Elements. *Appl. Opt.* **1998**, *37*, 4069−4079.

(17) Biagioni, P.; Huang, J.-S.; Hecht, B. Nanoantennas for Visible and Infrared Radiation. *Rep. Prog. Phys.* **2012**, *75*, 024402.

(18) Catchpole, K. R.; Polman, A. Design Principles for Particle Plasmon Enhanced Solar Cells. *Appl. Phys. Lett.* **2008**, *93*, 191113.

(19) Beck, F. J.; Verhagen, E.; Mokkapati, S.; Polman, A.; Catchpole, K. R. Resonant SPP Modes Supported by Discrete Metal Nanoparticles on High-index Substrates. *Opt. Express* **2011**, *19*, A146−A156.

(20) Temple, T. L.; Mahanama, G. D. K.; Reehal, H. S.; Bagnall, D. M. Influence of Localized Surface Plasmon Excitation in Silver Nanoparticles on the Performance of Silicon Solar Cells. *Sol. Energy Mater. Sol. Cells* **2009**, *93*, 1978−1985.